PROTEINS: Structure, Function, and Genetics 4:274–282 (1988)

Refined Structure of Human Carbonic Anhydrase II at 2.0 Å Resolution

A. Elisabeth Eriksson, T. Alwyn Jones, and Anders Liljas
Department of Molecular Biology, Biomedical Center, S-751 24 Uppsala, Sweden

ABSTRACT **The structure of human erythrocytic carbonic anhydrase II has been refined by constrained and restrained structure-factor least-squares refinement at 2.0 Å resolution. The conventional crystallographic R value is 17.3%. Of 167 solvent molecules associated with the protein, four are buried and stabilize secondary structure elements. The zinc ion is ligated to three histidyl residues and one water molecule in a nearly tetrahedral geometry. In addition to the zinc-bound water, seven more water molecules are identified in the active site. Assuming that Glu-106 is deprotonated at pH 8.5, some of the hydrogen bond donor–acceptor relations in the active site can be assigned and are described here in detail. The Oγ1 atom of Thr-199 donates its proton to the Oε1 atom of Glu-106 and can function as a hydrogen bond acceptor only in additional hydrogen bonds.**

Key words: crystallography, refinement, structure, carbonic anhydrase

INTRODUCTION

Human carbonic anhydrase II (HCA II) (carbonate dehydratase, EC 4.2.1.1) is a zinc enzyme with a molecular weight of 29,300. It is predominantly found in red blood cells where it catalyzes the reaction $CO_2 + H_2O \leftrightarrow HCO_3^- + H^+$ with a turnover rate of 10^6/seconds at pH 9, 25°C.[1,2] This high turnover rate makes HCA II one of the fastest enzymes known. The catalytic exchange CO_2/HCO_3^- has been thoroughly investigated and is described in a number of reviews.[3–6] One generally accepted scheme for catalysis involves a direct nucleophilic attack of the zinc bound hydroxyl ion on CO_2[3–6]:

$$Zn\text{–}OH^- + CO_2 \rightleftharpoons Zn\text{–}HCO_3^- \overset{+H_2O}{\rightleftharpoons} Zn\text{–}H_2O + HCO_3^- \quad \text{(step 1)}$$

$$Zn\text{–}H_2O + B \rightleftharpoons Zn\text{–}OH^- + BH^+ \quad \text{(step 2)}$$

B = buffer molecules

It has been suggested that the zinc-bound proton is not transferred directly to the external buffer in step (2), but through a rate-limiting proton transfer group, His-64,* on the enzyme.[2] This mechanism is supported both by kinetic data (for a review see ref. 8) and inhibition studies[9,10] where Cu^{2+} and Hg^{2+} ions inhibit the enzyme by binding to His-64. Recently, however, the role of His-64 has been tested by site-directed mutagenesis.[11] Mutants where the histidine has been replaced with either Lys, Glu, Gln, or Ala show only a slight reduction in the CO_2 hydration activity. These results indicate that His-64 is not essential for proton transfer since none of the substituted amino acids can function as an appropriate proton transfer group. Thus, the proton transfer in the catalytic mechanism of CA remains to be elucidated.[11]

The structure of human carbonic anhydrase II[12,13] has been refined at 2.0 Å resolution. This paper describes the refinement that gives a more accurate description of the structure, particularly of the hydrogen-bonding arrangement in the active site. This is of use for the continuing design and interpretation of site-directed mutagenesis experiments on the enzyme.

The structure of human carbonic anhydrase I (HCA I) has previously been refined at 2.0 Å resolution[14] and the structure of bovine CA III has recently been determined at 2.0 Å resolution (Eriksson and Liljas, manuscript in preparation).

MATERIALS AND METHODS

Crystallization, data collection, and determination of multiple isomorphous replacement (MIR) phase angles have been described elsewhere.[12] The crystals have space group $P2_1$ with cell dimensions a = 42.7 Å, b = 41.7 Å, c = 73.0 Å, and β = 104.6°. From the original precession film data set 15,770 reflections, corresponding to 94% of the total number of reflections to 2.0 Å, were used in the refinement. The starting coordinates were taken from the Protein Data Bank (Brookhaven, K.K. Kannan, 1976) and were rebuilt in the MIR map on a computer graphic system (Vector General 3400) using FRODO.[15,16] The resulting coordinates were first refined with the CORELS

Received September 6, 1988; accepted October 18, 1988.

Address reprint requests to Dr. A. Elisabeth Eriksson, Institute of Molecular Biology, University of Oregon, Eugene, OR 97403-1229.

Anders Liljas' present address is: Department of Molecular Biophysics, Chemical Center, University of Lund, Box 124, S-221 00 Lund, Sweden.

*The standard amino acid sequence for CA II[7] starts with number 2 and number 126 is deleted from the sequence.

TABLE I. Course of Model Building and Refinement

Resolution (Å)	No. of atoms	R*	Comments
2.0	2041	0.391	Model rebuilt on display, zinc atom and zinc-bound water molecule added
2.0	2041	0.257	Three cycles of CORELS. Overall thermal parameter = 15.0 Å^2
2.0	2150	0.207	Model rebuilt on display, 109 water molecules added. Three cycles of CORELS, group thermal parameters introduced
2.3	2150	0.195	Four cycles of PROLSQ, individual thermal parameters introduced
2.0	2196	0.184	Model rebuilt, 46 water molecules added, four cycles of PROLSQ
2.0	2199	0.179	Model rebuilt, three water molecules added, eight cycles of PROLSQ
2.0	2217	0.174	New water molecule identified in the active site. His-64 rotated, 18 water molecules added, six cycles of PROLSQ
2.0	2216	0.173	One water molecule deleted, four cycles of PROLSQ
2.0	2207	0.173	Nine water molecules deleted. Five cycles of PROLSQ

*Crystallographic residual $R = \Sigma||F_{obs}| - |F_{calc}||/\Sigma|F_{obs}|$.

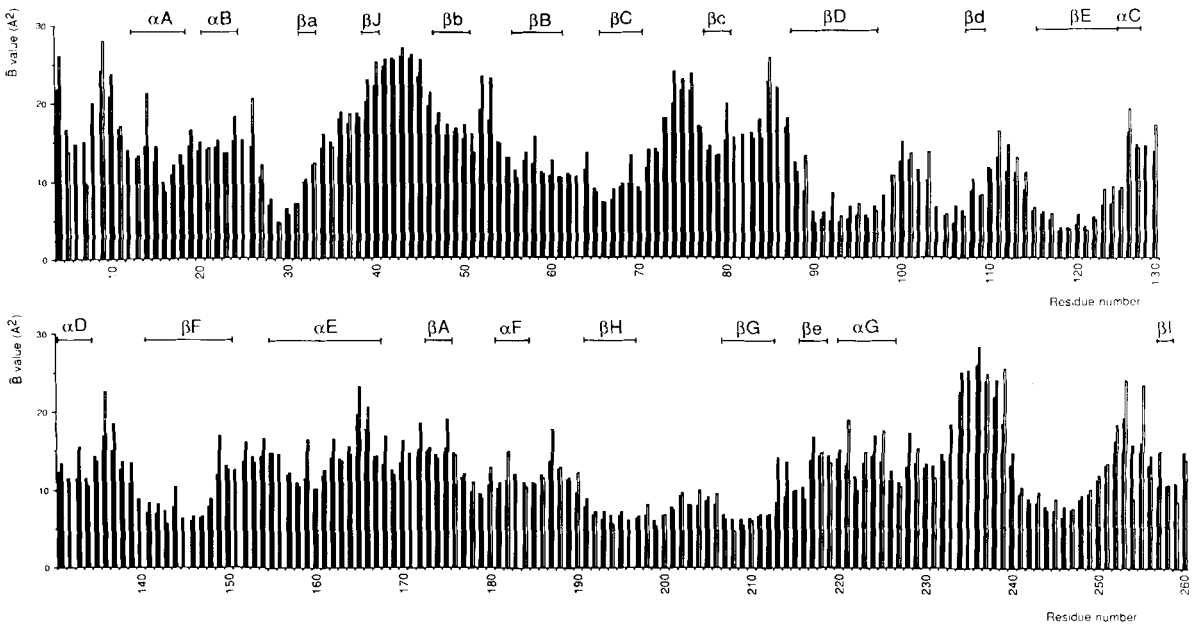

Fig. 1. Isotropic temperature factor (Å^2) variation of the HCA II polypeptide chain plotted as a function of residue number. The mean main chain and side chain B values are represented by the solid and open bars, respectively.

program system[17] and subsequently, to reduce the build up of restraint errors between peptides, with the PROLSQ program system[18] on a VAX 11/750 computer. At various stages during the refinement the atomic structure was checked against new $2|F_{obs}| - |F_{calc}|$ or $|F_{obs}| - |F_{calc}|$ Fourier maps using model phases. All data handling was done with PROTEIN[19] unless otherwise stated. Manual corrections of the atomic positions were made on an interactive graphics system (Vector General 3400 and Evans & Sutherland PS 300) using FRODO.

RESULTS AND DISCUSSION

Stereochemistry of the Model

The general course of the refinement is summarized in Table I. The final crystallographic R factor is 17.3% for data from 7.0 to 2.0 Å resolution. The root mean square (rms) departures from the restraints to ideal geometry in the final refinement cycle were 0.025, 0.038, and 0.040 Å for bond, angle, and fixed dihedral angle distances, respectively, 0.012 Å for out of plane restraints, and 0.150 Å^3 for chiral volumes.[18] The

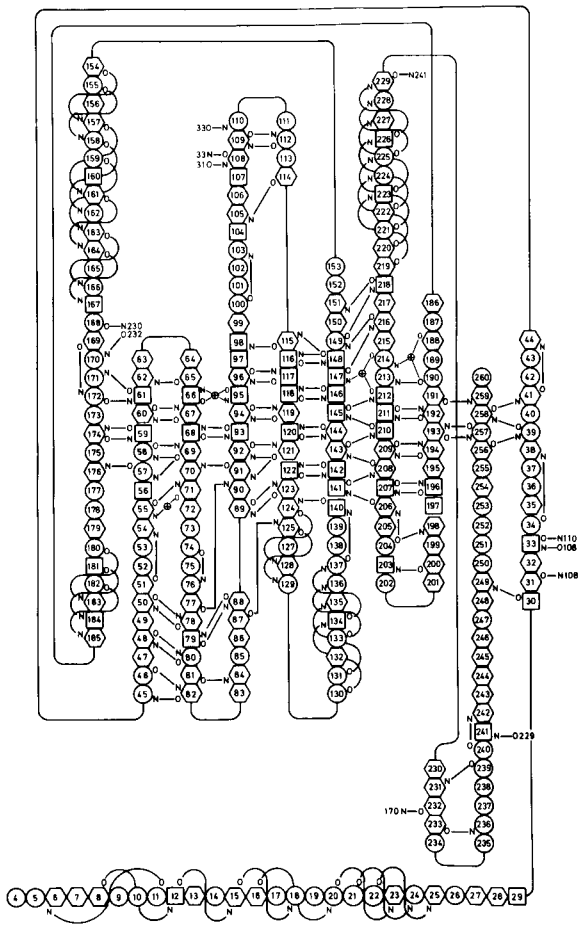

Fig. 2. Main chain hydrogen-bonding scheme of HCA II defined by DSSP.[20] The reader is referred to Table II for the nomenclature used to define different secondary structure elements. ⊕ indicates a water molecule buried and stabilizing secondary structure. The surface accessibility of different residues is illustrated as □, O Å^2; ⬡, 1–50 Å^2, and ○, >50 Å^2.

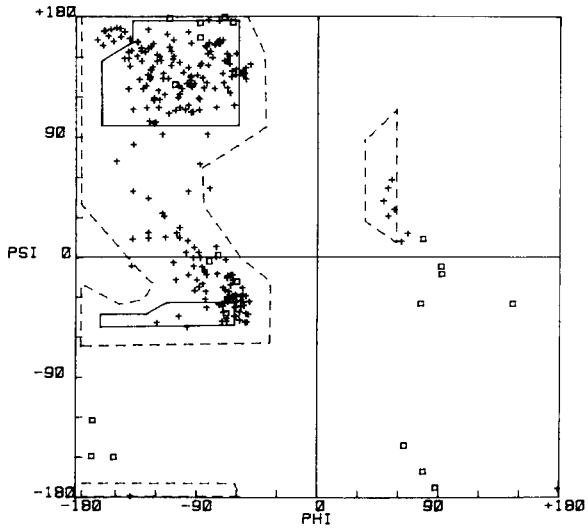

Fig. 3. Ramachandran plot of HCA II. Glycine residues are indicated by squares and nonglycines by crosses.

deviation from the isotropic thermal factor restraints were 0.785 Å^2 for main chain bonds, 1.306 Å^2 for main chain angles, 0.919 Å^2 for side chain bonds, and 1.527 Å^2 for the side chain angles. The rms parameter shifts in the final cycle were 0.016 Å for coordinates and 0.19 Å^2 for temperature factors.

The refined molecular model of HCA II is complete except for seven residues. We are unable to locate the N-terminal residues Ser-2 and His-3 and the C-terminal residue Lys-261. The electron density is weak for the entire residue Asn-253 and for the side chains of His-4, Lys-9, and Glu-14. Breaks of one grid point in the electron density at the main chain are observed at Ser-43 and Pro-237. Of 167 solvent molecules identified in the map all are within proper hydrogen bonding distances (less than 3.2 Å) to the protein and with refined temperature factors less than 50 Å^2. The refined coordinates are available from Protein Data Bank, Chemistry Department, Brookhaven National Laboratory, Upton, NY 11973 U.S.A.

The distribution of temperature factors over the individual residues is shown in Figure 1. The average temperature factors for the main chain atoms for individual residues vary between 3.2 to 26.1 Å^2. Residues with temperature factors over 20 Å^2 are situated on the surface of the protein with their side chains exposed to the solvent except for Leu-44 whose side chain is pointing inward.

Secondary structure elements in Table II were defined using the program DSSP.[20] The protein consists of three α-helices of which one starts and ends with a 3_{10}-helical conformation, four 3_{10}-helices, 14 turns (including turns of type I, II, II′, VIa, VIb[21–23]) and 15 β-strands. The hydrogen-bonding pattern of the main chain according to DSSP is shown in Figure 2. We used a cutoff value for the binding energy of less than −1.0 kcal/mol for hydrogen bonds. Of all the amino acids, 16% are in helical conformations and 28% in extended conformations. It is noteworthy that more than half of all helical residues are in 3_{10}-helical conformation.

The distribution of the ϕ and ψ torsion angles that define the polypeptide backbone of HCA II is illustrated in Figure 3 as a Ramachandran plot.[24] All the amino acids have allowed conformations. The seven residues in left-handed helical conformation are all situated in different links and turns on the main chain. These residues are Asp-110, Lys-111, Asn-178, Leu-203, Asp-243, Lys-252, and Asn-253.

General Shape of the Molecule

The structure of the protein is consistent with the model before refinement.[12,13] The molecule is an ellipsoid with dimensions 55 × 42 × 39 Å^3 at its extreme α-carbon positions. The folding of the enzyme is shown schematically in Figure 4 and the α-carbons

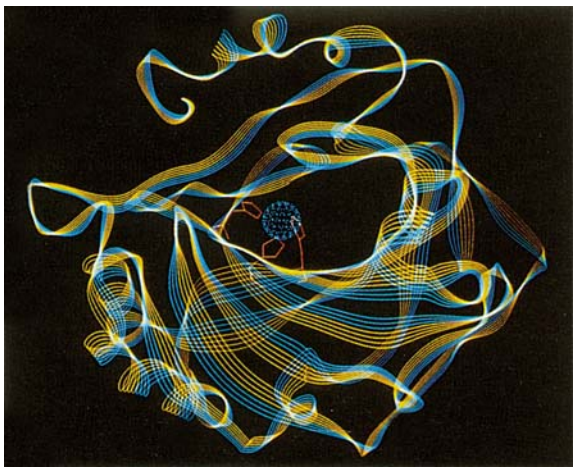

Fig. 4. Ribbon model of HCA II made with the graphic program BSRIBBON.[25] Added are the active site histidyl residues 94, 96, 119 and the zinc ion.

are shown in stereo in Figure 5. The previously described "knot" topology of the protein is maintained in the refinement, i.e., the protein will form a knot if the N-terminal and the C-terminal ends are pulled apart. This type of folding has not been observed for any other proteins.[26]

The molecule is divided into two halves by a 10-stranded twisted β-sheet structure; we have named the β-strands βA to βJ as seen from left to right with the molecule in its standard orientation (see Table II, Figs. 2 and 5). The lower half is built up of six pieces of polypeptide chain running almost perpendicularly to the central twisted β-sheet. Two of these strands are extensions of the βB and βC strands which, together with βD, form a smaller antiparallell β structure (βb, βc, and βD) on the surface of the protein. Three helices (αE, αF, and αG) are also part of this half of the protein. The upper half contains mainly the active site region and the N-terminal residues.

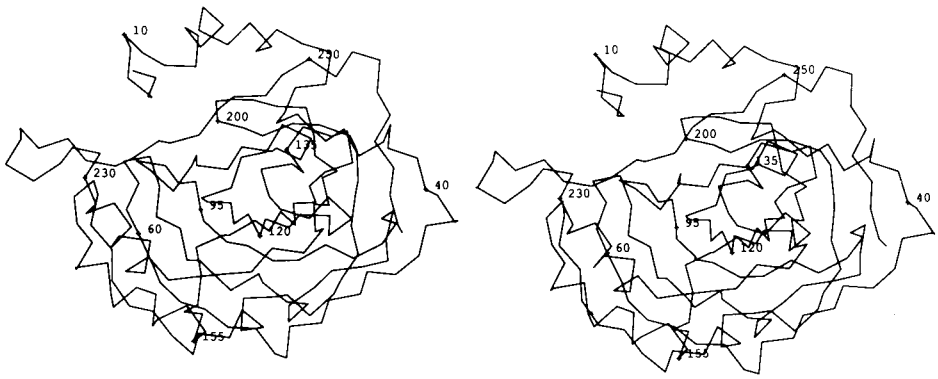

Fig. 5. Stereo drawing of an α-carbon backbone model of HCA II.

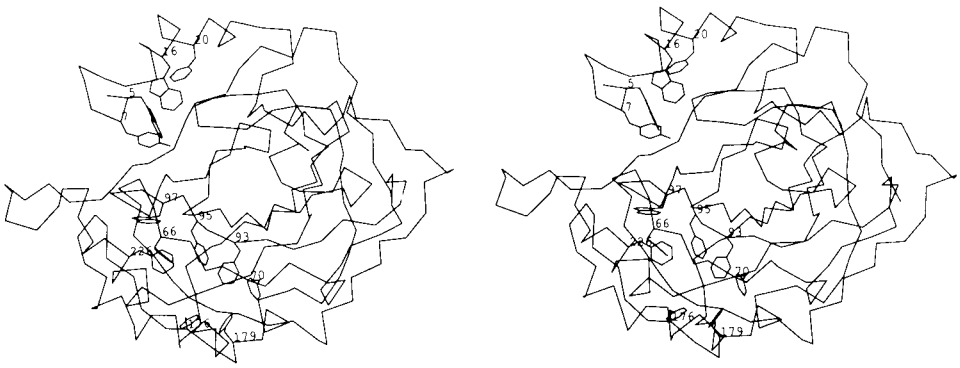

Fig. 6. Stereo drawing showing the two aromatic clusters in HCA II. One encloses Tyr-7 in the upper half of the molecule and includes Trp-5, Trp-16, and Phe-20. The second is situated at the lower half just below the zinc-binding histidines in the active site. This cluster includes the aromatic residues Phe-66, Phe-70, Phe-93, Phe-95, Phe-176, Phe-179, Phe-226, and Trp-97.

TABLE II. Secondary Structure of HCA II Defined by DSSP[20]*

α-Helix	3_{10}-helix	β-Strand	Turn	Residue number
	αA			13–18
	αB			21–24
			VIb (cis-Pro-30)	28–31
		βa		32–33
		βJ		39–40
		βb		47–50
		βB		56–61
		βC		66–70
		βc		78–81
			II′ (Gly-82)	81–84
		βD		88–97
		βd		108–109
		βE		116–124
	αC			125–128
αD				131–134
			I (Gln-136)	134–137
			I (Asp-139)	137–140
		βF		141–150
	αE			155–157
αE				158–163
	αE			163–167
		βA		173–175
	αF			181–184
		βH		191–196
			VIa (cis-Pro-202)	200–203
		βG		207–212
		βe		216–218
αG				220–226
			II (Gly-235)	233–236
		βI		257–258

*All specified turns are reversed turns as defined by Crawford et al. [21] except for VIb [22] which is an open turn. The 10 β-strands building the central twisted β-sheet structure are denoted with capital letters from one side of the sheet to the other.

TABLE III. Geometry of the Zinc Ion in HCA II*

	Distance (Å)	Angles (°)		
		X–Zn-94	X–Zn-96	X–Zn-119
OH^- 263	2.1	108	114	113
Nε2 94	2.0	—	107	114
Nε2 96	2.1	—	—	102
Nδ1 119	1.9	—	—	—

*No restraints were placed on the zinc coordination geometry during PROLSQ refinement.

The Hydrophobic Core

The lower half of the structure consists of an extensive hydrophobic core between the central β-sheet and the secondary structure elements on the surface. Thirty-four residues are involved in this core, of which 10 are aromatic. Eight of the aromatic residues are clustered together as has been observed in many other proteins.[27] These are phenylalanines 66, 70, 93, 95, 176, 179, and 226 and tryptophan 97 (see Fig. 6). These aromatic residues are conserved in both CA I and CA II and to a large extent also in CA III.[28] A number of aliphatic residues in the hydrophobic core are also conserved but to a lesser extent. It is noteworthy that Phe-93, Phe-95, and Trp-97 enclose the zinc ligands His-94 and His-96.

Also the upper half of the molecule has a smaller core of hydrophobic residues with an aromatic cluster involving four residues in the N-terminal region, Trp-5, Tyr-7, Trp-16, and Phe-20 (see Fig. 6). These residues are highly conserved in all available amino acid sequences of carbonic anhydrases.[28]

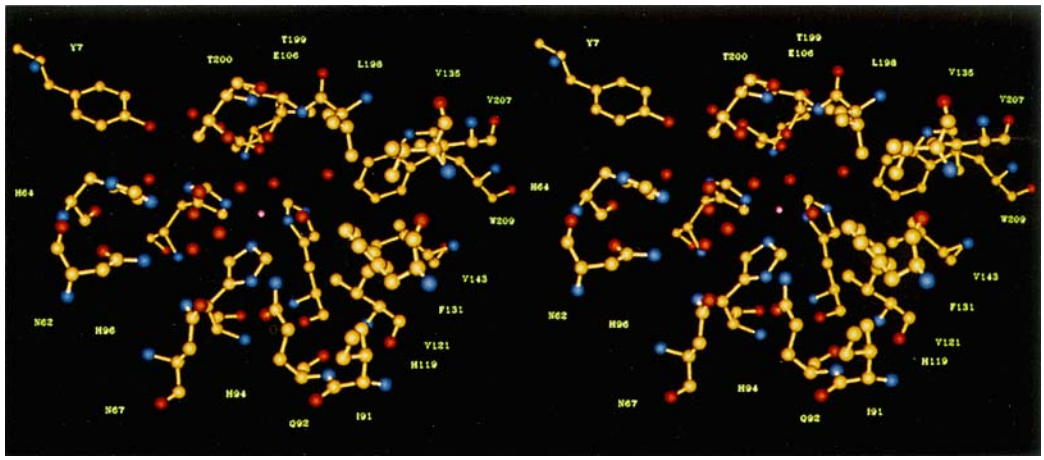

Fig. 7. Stereo drawing showing the active site of HCA II. Photograph is taken on a SUN 3/110 using the program FRODO PAINT (Mats Kihlén, Department of Molecular Biology, Uppsala University, Sweden).

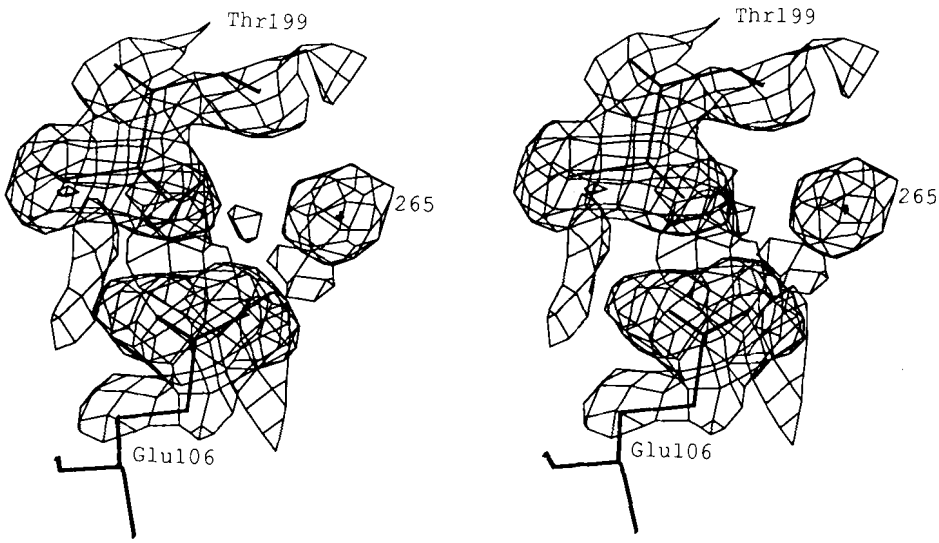

Fig. 8. Stereo views of the $2|F_{obs}| - |F_{calc}|$ difference map in part of the active site region of HCA II. Contours are drawn at height +1a where σ is the rms density throughout the unit cell.

The Active Site

The active site cavity of HCA II has a conical shape. It is about 15 Å wide at the entrance and penetrates about 15 Å into the middle of the molecule. The zinc ion is at the bottom of the cavity ligated to three histidyl residues (His-94, His-96, and His-119) that are situated on the βD and βE strands. The fourth ligand to the zinc ion is a water molecule (water 263). A pK_a value of 7.0 has been assigned to the zinc-bound water molecule[29] which must then be a hydroxyl ion at pH 8.5, which is the pH of the crystallization medium. The zinc coordination is almost tetrahedral; the distances and angles are shown in Table III. The histidines have very stable conformations as indicated by their low temperature factors (see Table IV and Fig. 1). Several factors contribute to this stability. The histidyl residues are situated on two neighboring β-strands in the middle of the major β-sheet structure and their second imidazole nitrogen atoms are hydrogen bonded to other residues: Nδ1 of His-94 to Oϵ1 of Gln-92, Nδ1 of His-96 to O of Asn-244 and Nδ2 of His-119 to Oϵ2 of Glu-117. Furthermore, three side chains of the β-strands on which the histidyl residues are located participate in a large aromatic cluster on the opposite side of the sheet, which probably contributes to the stability of the central residues.

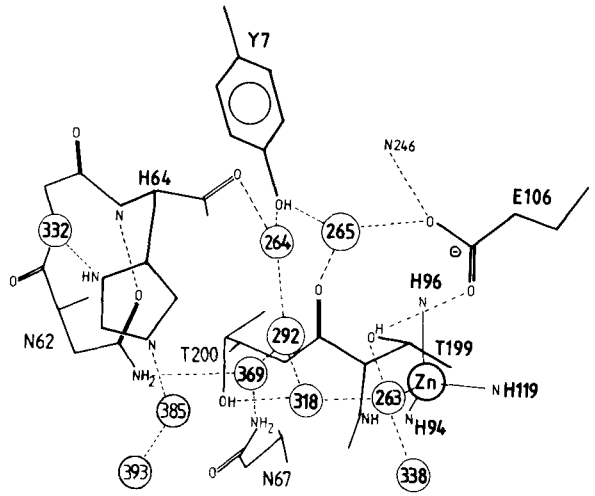

Fig. 9. Schematic drawing of the residues and water molecules in the active site of HCA II. Hydrogen bonds are indicated by dashed lines.

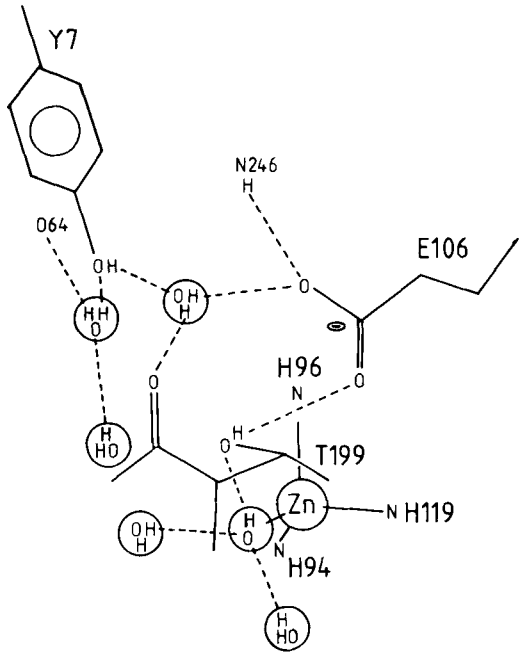

Fig. 10. Schematic drawing of the donor–acceptor relations in part of the hydrogen-bonding network in the active site of HCA II.

TABLE IV. Temperature Factors for Residue Side Chains and Water Molecules Within the Active Site*

Water or residue number	*B* value (Å^2)	Accessible surface (Å^2)
263 OHH	9.7	
264 OHH	13.1	
265 OHH	5.9	
292 OHH	22.8	
318 OHH	19.2	
332 OHH	28.5	
338 OHH	20.4	
369 OHH	16.6	
385 OHH	48.3	
393 OHH	32.8	
Tyr-7	9.3	27.0
Asn-62	11.0	33.0
His-64	14.2	48.0
Asn-67	8.4	17.0
Gln-92	7.9	31.0
His-94	6.9	22.0
His-96	4.1	2.0
Glu-106	6.7	1.0
Glu-117	5.4	0.0
His-119	3.4	2.0
Val-121	4.1	6.0
Phe-131	12.9	62.0
Val-135	13.1	20.0
Val-143	5.3	3.0
Leu-198	8.0	27.0
Thr-199	5.2	6.0
Thr-200	6.7	24.0
Val-207	6.2	0.0
Trp-209	4.9	1.0
Zn-262	8.2	0.4

*The temperature factors vary between 3.4 and 29.7 Å^2 for the side chain atoms in the protein structure. The table also includes solvent accessible surface[30] for the residues and the zinc ion.

TABLE V. Hydrogen-Bonding Distances in the Active Site of HCA II

Bond	Distance (Å)
263 OHH – 318 OHH	2.8
263 OHH – 338 OHH	2.7
263 OHH – Oγ1 Thr-199	2.8
264 OHH – 292 OHH	3.0
264 OHH – Oη Tyr-7	2.7
264 OHH – O His-64	3.0
265 OHH – Oη Tyr-7	2.4
265 OHH – Oε2 Glu-106	2.8
265 OHH – O Thr-199	3.0
292 OHH – 318 OHH	2.8
292 OHH – 369 OHH	2.7
318 OHH – Oγ1 Thr-200	2.9
332 OHH – Nδ1 His-64	3.1
369 OHH – Nδ2 Asn-62	2.8
369 OHH – Nδ2 Asn-67	2.8
385 OHH – 393 OHH	2.5
385 OHH – Nε2 His-64	2.6
Oδ1 Asn-62 – N His-64	3.0
Oε1 Gln-92 – Nδ1 His-94	2.7
Nδ1 His-96 – O Asn-244	2.7
Oε1 Glu-106 – Oγ1 Thr-199	2.4
Oε2 Glu-106 – N Ile-246	2.9
Oε2 Glu-117 – Nε2 His-119	2.6

Above the zinc ion the threonyl residues 199 and 200 are situated at the end of a long loop region, both more or less at the entrance of the cavity. On the opposite side of the cavity entrance, His-64 is found at the end of the βC strand. These residues together with Tyr-7, Asn-62, Asn-67, Gln-92, and Glu-106 form the hydrophilic side of the cavity. The other more hydrophobic side is built by the extension of strands βE and βF and the two short helices αC and αD situated on the loop between them. Residues in this region are Val-121, Phe-131, Val-135, Val-143, Leu-198, Val-207, and Trp-209. A stereo view of the active site is shown in Figure 7. Figure 8 shows the electron density of two central residues, Thr-199 and Glu-106, in the active site.

In addition to the zinc-bound hydroxyl ion, eight more water molecules were identified within the active site (numbers 264, 265, 292, 318, 338, 369, 385, and 393) forming a large hydrogen-bonding network leading to bulk water molecules (see Fig. 9). In addition water molecule 389 is in the vicinity, 3.5 Å from the Nε2 atom of Gln-92. Water molecule 338, referred to as the "deep" water, is situated in the deepest end of the active site and is 3.4 Å from the main chain N atom of Thr-199, which is involved in inhibitor and possibily also substrate binding.[10] The zinc-bound hydroxyl ion forms hydrogen bonds to the Oγ1 atom of Thr-199 and to water molecules 338 and 318. Water molecule 318 forms hydrogen bonds to the Oγ1 atom of Thr-200 and to water molecule 292, which in turn forms hydrogen bonds to two other water molecules (369 and 264), causing the water chain from the hydroxyl ion to branch. The three water molecules 264, 292, and 369, are situated 3.4–3.5 Å from the side chain of His-64.

Nitrogen assignment for the His-64 ring depends on water molecule 385. This has weak density and a temperature factor of 48 $Å^2$. However, this orientation of His-64 is in agreement with what has been observed in the crystal structures of the 3-acetoxymercuri-4-aminobenzenesulfonamide (AMS), SCN^-, and Hg^{2+}-inhibited enzymes where His-64 has a fixed conformation with its Nε2 atom toward the zinc ion.[10] With this orientation the Nδ1 atom also forms a good hydrogen bond to water molecule 332, which has no other hydrogen bond to the protein. The distance between the Nε2 atom of His-64 and the zinc-bound hydroxyl ion is 7.5 Å. The hydrogen-bonding distances in the active site are given in Table V. Oxygen and nitrogen assignment was possible for the side chains of Asn-62 and Gln-92 but not for the side chain of Asn-67.

Glu-106 and Glu-117 are two acidic residues buried (see Table IV) in the vicinity of the active site. Since hydrogen atoms cannot be seen in the electron density map, indirect arguments have to be used to discuss the probable charge state of these residues. In the case of trypsin, neutron diffraction analysis has shown that Asp-102 is not protonated despite its buried position,[31] and there are also other examples where buried charged residues have been solvated by uncharged hydrogen bond donor/acceptors from the protein.[32,33]

The Oε1 atom of Glu-117 is an acceptor for two hydrogen bonds from the main chain N atoms of Glu-106 and His-107 and the Oε2 atom is an acceptor for

two hydrogen bonds from Nδ1 of His-107 and Nε2 of His-119. The Oε2 atom of Glu-106 forms two hydrogen bonds to the main chain N atom of Arg-246 and water molecule 265, and the Oε1 atom forms one hydrogen bond to the Oγ1 atom of Thr-199. The large number of hydrogen bonds together with the high pH value of the crystallization medium (4 units above the normal pK_a for the glutamate carboxyl group) suggests that the two Glu carboxylic groups are negatively charged. With this assumption it is possible to assign the donor–acceptor relation of some hydrogen bonds in the active site. The proton of the Oγ1 atom of Thr-199 is donated to Glu-106. Thus the proton of the zinc-bound hydroxyl ion must be donated to Oγ1 of Thr-199 (see Fig. 10). This type of hydrogen-bonding scheme has also been suggested from the refined structure of HCA I.[14]

The possibility that the Oγ1 atom of Thr-199 can function only as hydrogen-bond acceptor for the solvent zinc ligand is a feature of crucial importance in the active site of HCA II. In the crystallographic studies of the AMS and SCN^--ion inhibited enzyme we have observed that the inhibitor molecules are restricted in their binding interaction with the zinc ion due to the proximity to Thr-199.[10] These results are presented in a subsequent article in this volume and form the basis for our modeling the substrate binding sites in HCA II.

ACKNOWLEDGMENTS

We are thankful for support and valuable discussions with Prof. Sven Lindskog, University of Umeå, Sweden. Dr. Torsten Unge at our institute is thanked for advice and assistance during the purification of native HCA II enzyme and Terese Bergfors for help with the manuscript. These studies have been supported by the Swedish Natural Science Research Council.

REFERENCES

1. Khalifah, R.G. The carbon dioxide hydration activity of carbonic anhydrase. J. Biol. Chem. 246:2561–2573, 1971.
2. Steiner, H., Jonsson, B.-H., Lindskog, S. The catalytic mechanism of carbonic anhydrase. Eur. J. Biochem. 59:253–259, 1975.
3. Pocker, Y., Sarkanen, S. Carbonic anhydrase: Structure, catalytic versatility, and inhibition. Adv. Enzymol. 47:149–274, 1978.
4. Lindskog, S. Carbonic anhydrase. Adv. Inorg. Biochem. 4:115–170, 1982.
5. Bertini, I., Luchinat, C., Scozzafava, A. Carbonic anhydrase: An insight into the zinc binding site and into the active cavity through metal substitution. Struct. Bonding 48:45–92, 1982.
6. Silverman, D.N., Vincent, S.H. Proton transfer in the catalytic mechanism of carbonic anhydrase. CRC Crit. Rev. Biochem. 14:207–255, 1983.
7. Henderson, L.E., Henriksson, D., Nyman, P.O. Primary structure of human carbonic anhydrase C. J. Biol. Chem. 251:5457–5463, 1976.
8. Silverman, D.N., Lindskog, S. The catalytic mechanism of carbonic anhydrase: Implications of a rate-limiting protolysis of water. Acc. Chem. Res. 21:30–36, 1988.
9. Tu, C., Wynns, G.C., Silverman, D.N. Inhibition by cupric ions of ^{18}O exchange catalyzed by human carbonic anhydarse II. J. Biol. Chem. 256:9466–9470, 1981.
10. Eriksson, A.E., Kylsten, P., Jones, T.A., Liljas A., Crystallographic studies of inhibitor binding sites in human carbonic anhydrase II: A penta-coordinated binding of the SCN^- ion to the zinc. Proteins 4:283–293, 1988. (The following article.)
11. Forsman, C., Behravan, G., Jonsson, B.-H., Liang, Z.-W., Lindskog, S., Ren, X., Sandstöm, J., Wallgren, K. Histidine 64 is not required for high CO_2 hydration activity of human carbonic anhydrase II. FEBS Lett. 229:360–362, 1988.
12. Liljas, A., Kannan, K.K., Bergstén, P.-C., Waara, I., Fridborg, K., Strandberg, B., Carlbom, U., Järup, L., Lövgren, S., Petef, M. Crystal structure of human carbonic anhydrase C. Nature New Biol. 235:131–137, 1972.
13. Nostrand, B., Vaara, I., Kannan, K.K. Structural relationship of human erythrocyte carbonic anhydrase isozymes B and C. In: "Isozymes I, Molecular Structure." Markert, C.L. ed. New York: Academic Press, 1975: 575–599.
14. Kannan, K.K., Ramanadham, M., Jones, T.A. Structure, refinement, and function of carbonic anhydrase isozymes: Refinement of human carbonic anhydrase I. Ann. N.Y. Acad. Sci. 429:49–60, 1984.
15. Jones, T.A., A graphics model building and refinement system for macromolecules. J. Appl. Crystallogr. 11:268–272, 1978..
16. Jones, T.A. FRODO: A graphics fitting program for macromolecules. In: "Computational Crystallography." Sayre, D. ed. Oxford: Clarendon Press, 1982: 303–317.
17. Sussman, J.L., Holbrook, S.R., Church, G.M., Kim, S.-H. A structure-factor least-squares refinement procedure for macromolecular structures using constrained and restrained parameters. Acta Crystallogr. A33:800–804, 1977.
18. Hendrickson, W.A., Konnert, J.H. Incorporation of stereochemical information into crystallographic refinement. In: "Computing in Crystallography." Diamond, R., Ramaseshan, S., Venkatesan, K. Eds. Bangalore: Indian Institute of Science, 1980: 13.01–13.23.
19. Steigeman, W., Die Entwicklung und Anwendung von Rechenverfahren und Rechenprogrammen zur Strukturanalyze von Proteinen am Beispiel des Trypsin-Trypsininhibitor Komplexes, des freien Inhibitors und der L-Asparaginase. Ph.D. thesis, Technical University, Munich, 1974.
20. Kabsch, W., Sander, C. Dictionary of protein secondary structure: Pattern recognition of hydrogen-bonded and geometrical features. Biopolymers 22:2577–2637, 1983.
21. Crawford, J.L., Lipscomb, W.N., Schellman, C.G. The reverse turn as a polypeptide conformation in globular proteins. Proc. Natl. Acad. Sci. U.S.A. 70:538–542, 1973.
22. Huber, R., Steigemann, W. Two cis-prolines in the Bence-Jones protein REI and the cis-Pro-bend. FEBS Lett. 48:235–237, 1974.
23. Richardson, J.S. The anatomy and taxonomy of protein structure. Adv. Prot. Chem. 34:167–339, 1981.
24. Ramachandran, G.N., Ramakrishnan, C., Sasisekharan, V. Stereochemistry of polypeptide chain conformations. J. Mol. Biol. 7:95–99, 1963.
25. Carson, M., Bugg, C.E. Algorithm for ribbon models of proteins. J. Mol. Graphics 4:121–122, 1986.
26. Creighton, T.E. "Proteins, Structures and Molecular Properties." New York: W.H. Freeman, 1983: 226.
27. Singh, J., Thornton, J.M. The interaction between phenylalanine rights in protein. FEBS Lett. 191:1–6, 1985.
28. Hewett-Emmett, D., Hopkins, P.J., Tashian, R.E., Czelusniak, J. Origins and molecular evolution of the carbonic anhydrase isozymes. Ann. N.Y. Acad. Sci. 429:338–358, 1984.
29. Lindskog, S., Engberg, P., Forsman, C., Ibrahim, S.A., Jonsson, B.-H., Simonsson, I., Tibell, L. Kinetics and mechanism of carbonic anhydrase isoenzymes. Ann. N.Y. Acad. Sci. 429:61–75, 1984.
30. Lee, B., Richards, F.M. The interpretation of protein structures: Estimation of static accessibility. J. Mol. Biol. 55:379–400, 1971.
31. Kossiakoff, A.A., Spencer, S.A. Direct determination of the protonation states of aspartic acid-102 and histidine-57 in the tetrahedral intermediate of the serine proteases: Neutron structure of Trypsin. Biochemistry 20:6462–6474, 1981.
32. Eklund, H., Jones, T.A., Schneider, G. Active site in alcohol dehydrogenease. In: "Zinc Enzymes." Bertini, I., Luchinat, C., Maret, W., Zeppezauer, M. eds. Boston, Basel, Stuttgart: Birkhäuser, 1986:377–392.
33. Quiocho, F.A., Sack, J.S., Vyas, N.K. Stabilization of charges on isolated ionic groups sequestered in proteins by polarized peptide units. Nature 329:561–564, 1987.